TAILORED FINITE POINT METHOD FOR THE INTERFACE PROBLEM

ZHONGYI HUANG

Dept. of Mathematical Sciences
Tsinghua University, Beijing 100084, China

(Communicated by Kenneth Karlsen)

ABSTRACT. In this paper, we propose a tailored-finite-point method for a numerical simulation of the second order elliptic equation with discontinuous coefficients. Our finite point method has been tailored to some particular properties of the problem, then we can get the approximate solution with the same behaviors as that of the exact solution very naturally. Especially, in one-dimensional case, when the coefficients are piecewise linear functions, we can get the *exact solution* with only one point in each subdomain. Furthermore, the *stability analysis* and the *uniform convergence analysis* in the energy norm are proved. On the other hand, our computational complexity is only $\mathcal{O}(N)$ for N discrete points. We also extend our method to two-dimensional problems.

1. **Introduction.** The elliptic and parabolic problems with discontinuous coefficients arise in many fields, such as material sciences, physical geography, multiphase fluid dynamics or fluid-solid interactions, and so on. In general, although the solution of the interface problem is smooth in each subdomain occupied by single kind of material or fluid, the global regularity of the solution may be poor, it may have singularities at the interfaces (*cf.* [1, 2, 8, 9]). Because the singularities at different interfaces may be different, and the geometry of the interfaces are usually quite complex in practice, using the traditional finite element or finite difference methods are not easily to achieve high accuracy in these cases.

Babuška [1, 2] studied the elliptic interface problem defined on a smooth domain with a smooth interface. The author used the finite element method to solve the equivalent minimization problems and obtained the energy-norm error estimates. Furthermore, Babuška et al [3] studied the approximation of a class of second order elliptic problems with rough coefficients. They used some special finite elements which were chosen to accurately model the unknown solution.

Han [10] proposed an infinite element method for elliptic interface problems in two dimensional with interfaces consisting of straight lines. This method may be considered as a certain scheme of mesh refinement but can be implemented more easily. The first order energy-norm error estimate was achieved in [10].

Chen and Zou [6] considered the fitted finite-element method for solving second-order elliptic and parabolic interface problems, and the error estimates of order

$O(h^2|\log h|)$ in the L^2-norm and of order $O(h\sqrt{|\log h|})$ in the energy norm were proved. R. K. Sinha and B. Deka [21] proposed an unfitted finite element method for the elliptic and parabolic interface problems. They achieved the first order convergence rate in the energy norm and the order of $O(h^2|\log h|)$ in the L^2-norm.

Barrett and Elliott [4] analyzed the elliptic interface problems via a penalty method. They proved that the approximate solution has an optimal convergent rate in both the H^1-norm and the L^2-norm, on any interior domain, under an appropriate choosing of the penalty parameter.

LeVeque and Li [14] proposed an immersed interface method for elliptic interface problems defined on a regular domain for which a uniform grid can be used. This method achieves a second order accuracy in L^2-norm by incorporating the interface conditions into the finite difference schemes. They also used this method to some other problems. The convergence and the stability of the IIM has been proved in [15, 16].

Wei et al [22, 23] introduced the matched interface and boundary (MIB) method, for solving elliptic equations with discontinuous coefficients and singular sources. For elliptic problems with sharp-edged interfaces, their numerical experiments confirm the designed second order convergence of the proposed method. But they did not prove the stability, thus the convergence cannot be established.

If the interface problem has some symmetric properties, for example, if it is axial symmetry, we can reduce the original problem to one-dimensional. We will study the high dimensional problems by our method later. Let us start with the numerical solutions of interface problems as follows:

$$-\big(a(x)u'(x)\big)' + b(x)u(x) = f(x), \quad \forall x \in \Omega \setminus x_0, \tag{1}$$

$$u|_{\partial\Omega} = 0, \tag{2}$$

$$[u]|_{x_0} = \alpha, \quad [au']|_{x_0} = \beta, \tag{3}$$

where $\Omega = (c,d) \subset \mathbb{R}$, $f \in L^2(\Omega)$, $\alpha, \beta \in \mathbb{R}$, $a(x)$ and $b(x)$ are two piecewise smooth functions, $s.t.$

$$0 < a_0 \le a(x) \le A_0 < \infty, \qquad 0 \le b(x) \le B_0 < \infty; \tag{4}$$

$[v]|_{x_0}$ is the jump of a quantity v at the point x_0, $i.e.$ $[v]|_{x_0} = v(x_0^+) - v(x_0^-)$, where $v(x_0^\pm)$ means the limitation of $v(x)$ as x goes to x_0 from the right/left hand side of x_0.

For our model problem (1)–(3), if we let

$$y(x) = \int_c^x \frac{1}{a(\xi)} d\xi, \quad \text{for } x \in \Omega, \tag{5}$$

$$y_0 = y(x_0), \quad d_0 = y(d), \quad D_1 = (0, y_0), \quad D_2 = (y_0, d_0), \quad D = (0, d_0),$$
$$c(y) \equiv a\big(x(y)\big)b\big(x(y)\big), \quad F(y) \equiv a\big(x(y)\big)f\big(x(y)\big),$$

then the function $U(y) \equiv u\big(x(y)\big)$ shall satisfy the following problem:

$$-U''(y) + c(y)U(y) = F(y), \quad \text{for } y \in D \setminus y_0, \tag{6}$$

$$U|_{\partial D} = 0, \tag{7}$$

$$[U]|_{y_0} = \alpha, \quad [U']|_{y_0} = \beta. \tag{8}$$

In this paper, we propose an approach which is based on the properties of the locally approximate problem to solve our interface problem (6)–(8). Our method

can give a natural approximation of the solution to the original problem with its essential properties, such as the boundary layers and interior layers.

The rest part of this paper is organized as follows. In section 2, we discuss the analytic stability results for our model problem (6)–(8). In section 3, we present our tailored-finite-point method for the interface problem based on the properties of the solutions. We also prove the stability analysis and error estimates for our numerical method and extend it to two dimensional problems. In section 4, some numerical examples are given to show the efficiency of our method. Finally, we make a short conclusion in section 5.

2. **Analytical stability analysis.** We shall first introduce some notations used in this paper. Let

$$L^2(D) = \left\{ v \,\middle|\, \int_D |v(y)|^2 dy < +\infty \right\}$$

denote the space of all square-integrable functions equipped with the inner product

$$(v, w) := \int_D v(y)\bar{w}(y)dy$$

and the norm

$$\|v\|_{0,D} := \sqrt{(v, v)}.$$

We also introduce the Sobolev spaces, for $l \in \mathbb{N}$,

$$H_*^l(D) = \left\{ v \in L^2(D) \,\middle|\, v|_{\partial D} = 0, \ v^{(j)}|_{D_k} \in L^2(D_k), \ j = 1, \cdots, l, \ k = 1, 2 \right\},$$

where $v^{(j)}$ are the derivatives of order j in the distribution sense. By

$$|v|_{l,D}^* := \sqrt{\|v^{(l)}\|_{0,D_1}^2 + \|v^{(l)}\|_{0,D_2}^2}$$

a semi-norm is given in $H_*^l(D)$. A norm of the space $H_*^l(D)$ is defined as

$$\|v\|_{l,D}^* = \left(\sum_{j=0}^{l} \left(|v|_{j,D}^* \right)^2 \right)^{1/2}.$$

From now on, if not stated otherwise, all constants C, or C_j, with $j \in \mathbb{N}$, are assumed to be independent of all parameters of the given estimate, and having, in general, different meanings in different contexts. Furthermore, we suppose that

$$F \in L^2(D), \quad c \in L^\infty(D). \tag{9}$$

We then have the following estimates for our interface problem (6)–(8).

Lemma 2.1. (Stability analysis for analytic solution) *Suppose the conditions (9) hold, U is the solution of (6)-(8). Then $U \in H_*^2(D)$ and the following estimate*

$$\|U\|_{2,D}^* \leq C\left(\|F\|_{0,D} + |\alpha| + |\beta| \right), \tag{10}$$

holds for a positive constant C which is independent of F, α and β.

Proof. Multiplying (6) by U and integrating over $D_1 \bigcup D_2$ yields

$$\alpha U'(y_0^-) + \beta U(y_0^+) + \int_{D_1 \cup D_2} \left(|U'|^2 + c|U|^2 \right) dy = \int_D FU \, dy.$$

By Poincaré's inequality and Young's inequality, we have

$$C \left(\|U\|_{1,D}^* \right)^2 \leq \int_{D_1 \cup D_2} \left(|U'|^2 + c|U|^2 \right) dy = \int_D FU \, dy - \alpha U'(y_0^-) - \beta U(y_0^+)$$

$$\leq \quad \frac{1}{2\varepsilon_1} \|F\|_{0,D}^2 + \frac{\varepsilon_1}{2} \|U\|_{0,D}^2 + |\alpha| \cdot |U'(y_0^-)| + |\beta| \cdot |U(y_0^+)|, \quad \forall \varepsilon_1 > 0. \qquad (11)$$

Furthermore, from the equation (6) and the conditions (9), we get

$$U(y_0^+) \quad = \quad \int_{d_0}^{y_0} U'(y) \, dy,$$

$$U'(y_0^-) \quad = \quad U'(y) + \int_y^{y_0} U''(z) \, dz = U'(y) + \int_y^{y_0} \left(cU - F \right)(z) \, dz, \quad \forall y \in (0, y_0).$$

By Cauchy-Schwartz inequality and Young's inequality, we obtain

$$|\beta| \left| U(y_0^+) \right| = |\beta| \left| \int_{d_0}^{y_0} U'(y) \, dy \right| \leq |\beta| \int_{y_0}^{d_0} |U'(y)| \, dy$$

$$\leq \quad \sqrt{d_0 - y_0} |\beta| \cdot |U|_{1,D_2} \leq \frac{1}{2\varepsilon_2} (d_0 - y_0) |\beta|^2 + \frac{\varepsilon_2}{2} |U|_{1,D_2}^2, \quad \forall \varepsilon_2 > 0,$$

$$|\alpha| \left| U'(y_0^-) \right| = \frac{|\alpha|}{y_0} \left| \int_0^{y_0} U'(y_0^-) dy \right|$$

$$= \quad \frac{|\alpha|}{y_0} \left| \int_{D_1} \left(U'(y) + \int_y^{y_0} \left(cU - F \right)(z) \, dz \right) dy \right|$$

$$\leq \quad \frac{|\alpha|}{y_0} \int_{D_1} \left| U'(y) + \int_y^{y_0} \left(cU - F \right)(z) \, dz \right| dy$$

$$\leq \quad \frac{|\alpha|}{\sqrt{y_0}} |U|_{1,D_1} + |\alpha| \sqrt{y_0} \left(A_0 B_0 \|U\|_{0,D_1} + \|F\|_{0,D_1} \right)$$

$$\leq \quad \frac{|\alpha|^2}{2 y_0 \varepsilon_3} + \frac{\varepsilon_3}{2} |U|_{1,D_1}^2 + \frac{|\alpha|^2 A_0^2 B_0^2 y_0}{2\varepsilon_4} + \frac{\varepsilon_4}{2} \|U\|_{0,D_1}^2 + \frac{|\alpha|^2 y_0 + \|F\|_{0,D_1}^2}{2},$$

$$\forall \varepsilon_3, \varepsilon_4 > 0.$$

Substituting the above inequalities into (11), choose $\varepsilon_1, \varepsilon_2, \varepsilon_3, \varepsilon_4$ small enough, we obtain

$$\left(\|U\|_{1,D}^* \right)^2 \leq C \left(\|F\|_{0,D}^2 + |\alpha|^2 + |\beta|^2 \right). \qquad (12)$$

Furthermore, by (6), we have

$$\left(\|U\|_{2,D}^* \right)^2 \quad = \quad \left(\|U\|_{1,D}^* \right)^2 + |U|_{2,D_1}^2 + |U|_{2,D_2}^2 = \left(\|U\|_{1,D}^* \right)^2 + \int_D |cU - F|^2 dy$$

$$\leq \quad \left(\|U\|_{1,D}^* \right)^2 + C(\|F\|_{0,D}^2 + \|U\|_{0,D}^2). \qquad (13)$$

Then we get (10) from (12)–(13) immediately. □

3. **Finite point method.** In this section, we present a new approach to construct the discrete scheme for the interface problem (6)–(8). We call the new scheme a "**tailored finite point method**" (TFPM) [11, 12], because the finite point method has been tailored to some particular properties or solutions of the problem. The finite point method [7, 17, 18, 20] is a development of finite difference method, in which the meshless technique is emphasized. For one dimensional singular perturbation problem, the method is very close to the method of "exponential fitting" discussed in [5, 13, 19].
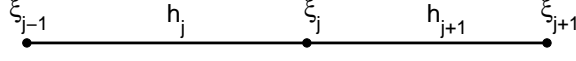
FIGURE 1. The local mesh around points ξ_{j-1}, ξ_j, and ξ_{j+1}.

3.1. **TFPM for interface problem.** We now want to construct a tailored finite-point scheme for the elliptic equation (6). Without loss of any generality, we assume that the computational domain is $D = (0, 1)$ and the interface is at $y = y_0$. First, we take a partition as (*cf.* Figure 1):

$$0 = \xi_0 < \xi_1 < \cdots < \xi_N = 1,$$

with

$$h_j = \xi_j - \xi_{j-1}, \quad j = 1, 2, \cdots, N, \quad \text{and} \quad h = \max_{1 \leq j \leq N} h_j,$$

such that $c(y)$ is smooth on each subdomain $D_j = (\xi_{j-1}, \xi_j)$. Suppose that $\xi_{n_0} = y_0$. Then we approximate the coefficient $c(y)$ by piecewise linear function, *i.e.* we introduce an approximate function $c_h(y)$ for $c(y)$, *s.t.*

$$\left. \begin{array}{l} c_h(y) = a_j y + b_j, \quad \text{for } y \in D_j, \\ c_h(\xi_{j-1}^+) = c(\xi_{j-1}^+), \quad c_h(\xi_j^-) = c(\xi_j^-), \end{array} \right\} \quad j = 1, \cdots, N.$$

Now we obtain an approximate problem of (6)–(8) for U_h,

$$-U_h'' + c_h U_h = F, \qquad \forall y \in D_j, \; j = 1, \cdots, N, \tag{14}$$

$$U_h(0) = U_h(1) = 0, \tag{15}$$

$$U_h(\xi_j^-) = U_h(\xi_j^+), \quad U_h'(\xi_j^-) = U_h'(\xi_j^+), \quad 1 \leq j \leq N - 1, \text{ and } j \neq n_0, \tag{16}$$

$$U_h(\xi_{n_0}^-) = U_h(\xi_{n_0}^+) - \alpha, \quad U_h'(\xi_{n_0}^-) = U_h'(\xi_{n_0}^+) - \beta. \tag{17}$$

For $j = 1, \cdots, N$, we have three cases:

• If $a_j = b_j = 0$, let

$$G_j(y, s) = \begin{cases} s - y, & y \geq s, \\ 0, & s \geq y. \end{cases} \tag{18}$$

Then the solution of (14) in D_j can be expressed by

$$U_h(y) = A_j + B_j y + \int_{\xi_{j-1}}^{\xi_j} F(s) G_j(y, s) ds, \quad \text{for } y \in D_j, \tag{19}$$

with two constants $A_j, B_j \in \mathbb{R}$. Let

$$\lambda_j^+ = \lambda_j^- = 1, \quad \gamma_j^+ = \gamma_j^- = 0, \quad \mu_j^+ = \xi_j, \quad \mu_j^- = \xi_{j-1}, \quad \delta_j^+ = \delta_j^- = 1, \tag{20}$$

$$F_j^+ = \int_{\xi_{j-1}}^{\xi_j} F(s)(s - \xi_j) ds, \quad F_j^- = 0, \quad G_j^+ = -\int_{\xi_{j-1}}^{\xi_j} F(s) ds, \quad G_j^- = 0. \tag{21}$$

• If $a_j = 0$, $b_j \neq 0$, let

$$\hat{G}_j(y, s) = \frac{1}{2\sqrt{b_j}} \begin{cases} \sinh \sqrt{b_j}(s - y), & y \geq s, \\ \sinh \sqrt{b_j}(y - s), & s \geq y. \end{cases} \tag{22}$$

Then the solution of (14) in D_j can be expressed by

$$U_h(y) = A_j e^{y\sqrt{b_j}} + B_j e^{-y\sqrt{b_j}} + \int_{\xi_{j-1}}^{\xi_j} F(s) \hat{G}_j(y, s) ds, \quad \text{for } y \in D_j, \tag{23}$$

with two constants $A_j, B_j \in \mathbb{R}$. Let

$$\lambda_j^+ = e^{\xi_j \sqrt{b_j}}, \quad \lambda_j^- = e^{\xi_{j-1} \sqrt{b_j}}, \quad \gamma_j^+ = \sqrt{b_j}\, e^{\xi_j \sqrt{b_j}}, \quad \gamma_j^- = \sqrt{b_j}\, e^{\xi_{j-1} \sqrt{b_j}},$$

$$\mu_j^+ = e^{-\xi_j \sqrt{b_j}}, \quad \mu_j^- = e^{-\xi_{j-1} \sqrt{b_j}},$$

$$\delta_j^+ = -\sqrt{b_j}\, e^{-\xi_j \sqrt{b_j}}, \quad \delta_j^- = -\sqrt{b_j}\, e^{-\xi_{j-1} \sqrt{b_j}},$$

$$F_j^+ = \int_{\xi_{j-1}}^{\xi_j} F(s)\hat{G}_j(\xi_j, s)ds, \quad G_j^+ = \int_{\xi_{j-1}}^{\xi_j} F(s)\partial_y \hat{G}_j(y, s)\big|_{y=\xi_j} ds, \qquad (24)$$

$$F_j^- = \int_{\xi_{j-1}}^{\xi_j} F(s)\hat{G}_j(\xi_{j-1}, s)ds, \quad G_j^- = \int_{\xi_{j-1}}^{\xi_j} F(s)\partial_y \hat{G}_j(y, s)\big|_{y=\xi_{j-1}} ds. \qquad (25)$$

• If $a_j \neq 0$, let

$$z(y) = (a_j)^{-\frac{2}{3}}(a_j y + b_j), \quad z_{j-1} = z(\xi_{j-1}), \quad z_j = z(\xi_j),$$
$$\widetilde{F}(s) = (a_j)^{-\frac{2}{3}} F\left((a_j)^{-\frac{1}{3}}s - \frac{b_j}{a_j}\right),$$

$$\widetilde{G}_j(t, s) = -\frac{1}{2}\left\{ \begin{array}{ll} \mathrm{Ai}(s)\mathrm{AI}(t) + \mathrm{Bi}(s)\mathrm{BI}(t), & t \geq s, \\ \mathrm{Ai}(s)\mathrm{AI}(s) + \mathrm{Bi}(s)\mathrm{BI}(s), & s \geq t, \end{array} \right. \qquad (26)$$

where $\mathrm{Ai}(s)$ and $\mathrm{Bi}(s)$ are the Airy functions of the first and the second kind respectively, and

$$\mathrm{AI}(t) = \int_0^t \big(\mathrm{Ai}(\eta)\big)^{-2} d\eta, \quad \mathrm{BI}(t) = \int_0^t \big(\mathrm{Bi}(\eta)\big)^{-2} d\eta.$$

Then the solution of (14) in D_j can be expressed by

$$U_h\big(z(y)\big) = A_j \mathrm{Ai}\big(z(y)\big) + B_j \mathrm{Bi}\big(z(y)\big) + \int_{z_{j-1}}^{z_j} \widetilde{F}(s)\widetilde{G}_j\big(z(y), s\big)ds, \ \forall y \in D_j, \quad (27)$$

with two constants $A_j, B_j \in \mathbb{R}$. Let

$$\lambda_j^+ = \mathrm{Ai}\big(z(\xi_j)\big), \ \lambda_j^- = \mathrm{Ai}\big(z(\xi_{j-1})\big),$$
$$\gamma_j^+ = (a_j)^{\frac{1}{3}}\mathrm{Ai}'\big(z(\xi_j)\big), \ \gamma_j^- = (a_j)^{\frac{1}{3}}\mathrm{Ai}'\big(z(\xi_{j-1})\big),$$
$$\mu_j^+ = \mathrm{Bi}\big(z(\xi_j)\big), \ \mu_j^- = \mathrm{Bi}\big(z(\xi_{j-1})\big),$$
$$\delta_j^+ = (a_j)^{\frac{1}{3}}\mathrm{Bi}'\big(z(\xi_j)\big), \ \delta_j^- = (a_j)^{\frac{1}{3}}\mathrm{Bi}'\big(z(\xi_{j-1})\big),$$

$$F_j^+ = \int_{z_{j-1}}^{z_j} \widetilde{F}(s)\widetilde{G}_j\big(z(\xi_j), s\big)ds, \quad G_j^+ = \int_{z_{j-1}}^{z_j} \widetilde{F}(s)\partial_y \widetilde{G}_j\big(z(y), s\big)\big|_{y=\xi_j} ds, \quad (28)$$

$$F_j^- = \int_{z_{j-1}}^{z_j} \widetilde{F}(s)\widetilde{G}_j\big(z(\xi_{j-1}), s\big)ds, \quad G_j^- = \int_{z_{j-1}}^{z_j} \widetilde{F}(s)\partial_y \widetilde{G}_j\big(z(y), s\big)\big|_{y=\xi_{j-1}} ds. (29)$$

From (15)–(17), we have

$$\lambda_1^- A_1 + \mu_1^- B_1 + F_1^- = 0, \qquad \lambda_N^+ A_N + \mu_N^+ B_N + F_N^+ = 0, \qquad (30)$$

$$\left\{ \begin{array}{l} \lambda_j^+ A_j + \mu_j^+ B_j + F_j^+ = \lambda_{j+1}^- A_{j+1} + \mu_{j+1}^- B_{j+1} + F_{j+1}^-, \\ \gamma_j^+ A_j + \delta_j^+ B_j + G_j^+ = \gamma_{j+1}^- A_{j+1} + \delta_{j+1}^- B_{j+1} + G_{j+1}^-, \end{array} \right. \quad j \neq n_0, \qquad (31)$$

$$\left\{ \begin{array}{l} \lambda_{n_0}^+ A_{n_0} + \mu_{n_0}^+ B_{n_0} + F_{n_0}^+ = \lambda_{n_0+1}^- A_{n_0+1} + \mu_{n_0+1}^- B_{n_0+1} + F_{n_0+1}^- - \alpha, \\ \gamma_{n_0}^+ A_{n_0} + \delta_{n_0}^+ B_{n_0} + G_{n_0}^+ = \gamma_{n_0+1}^- A_{n_0+1} + \delta_{n_0+1}^- B_{n_0+1} + G_{n_0+1}^- - \beta. \end{array} \right. \quad (32)$$

Now we obtain a linear system (30)–(32) of $2N$ equations for $2N$ unknowns $\{A_j, B_j, j = 1, \cdots, N\}$. Solving this linear system, we can get our approximate solution $U_h(y)$.

Remark 1. Certainly, in practice, we need some quadrature rules to get the integrals in (21), (24)–(25) and (28)–(29). In general, if we approximate F by piecewise polynomials or piecewise trigonometric functions, we can get these integrals explicitly with high accuracy.

Remark 2. It is easy to solve our linear system (30)–(32). From (31)–(32), we have

$$\begin{pmatrix} A_j \\ B_j \end{pmatrix} = \begin{pmatrix} \zeta_j & \eta_j \\ \xi_j & \theta_j \end{pmatrix} \begin{pmatrix} A_{j+1} \\ B_{j+1} \end{pmatrix} + \begin{pmatrix} v_j \\ \omega_j \end{pmatrix}, \quad j = 1, \cdots, N-1,$$

with some constants $\zeta_j, \eta_j, \xi_j, \theta_j, v_j, \omega_j$, and $\zeta_j\theta_j - \xi_j\eta_j \neq 0$, for $j = 1, \cdots, N-1$. Then we get

$$\begin{pmatrix} A_1 \\ B_1 \end{pmatrix} = \begin{pmatrix} \zeta & \eta \\ \xi & \theta \end{pmatrix} \begin{pmatrix} A_N \\ B_N \end{pmatrix} + \begin{pmatrix} v \\ \omega \end{pmatrix},$$

with some constants $\zeta, \eta, \xi, \theta, v, \omega$ by iteration. Then, combining with (30), we can get A_1, B_1, A_N, B_N immediately. Finally, we can obtain A_j, B_j $(j = 2, \cdots, N-1)$ by recursion. The computational complexity for solving the linear system (30)–(32) is $\mathcal{O}(N)$.

3.2. **Convergence analysis of TFPM.** We now turn to the convergence analysis of our method. From now on, we suppose that $c(\cdot)|_{D_j} \in C^2(\bar{D}_j)$, $j = 1, \cdots, N$. From the definition of c_h, we have

$$|c(y) - c_h(y)| \leq \mathcal{M}h^2, \qquad \forall y \in D, \tag{33}$$

with

$$\mathcal{M} = \frac{1}{2} \max_{1 \leq j \leq N} \max_{y \in D_j} |c''(y)| < +\infty.$$

Suppose that U is the solution of problem (6)–(8), and U_h is the solution of (14)–(17). Let us denote by

$$E(y) \equiv U(y) - U_h(y), \qquad R_h \equiv (c_h - c)U. \tag{34}$$

We then obtain

$$-E''(y) + c_h E(y) = R_h(y), \quad y \in D, \tag{35}$$

$$E(0) = 0, \qquad E(1) = 0, \tag{36}$$

$$E \quad \text{and} \quad E' \quad \text{are continuous on } D. \tag{37}$$

Lemma 3.1. (Stability analysis for TFPM) *Suppose $F \in L^2(D)$, $c(\cdot)|_{D_j} \in C^2(\bar{D}_j)$, $(j = 1 \cdots, N)$. Then we have $E \in H_*^2(D)$ and the following estimate*

$$\|E\|_{2,D}^* \leq C\|R_h\|_{0,D}, \tag{38}$$

with a constant C independent of R_h.

Proof. As $F \in L^2(D)$ and $c(y)$ is also piecewise smooth on D, we know c_h is piecewise smooth on D, and $R_h \in L^2(D)$. Then we obtain (38) from Lemma 2.1 immediately. $\square$

Theorem 3.2. (Error estimate for TFPM) *The following error estimate*

$$\|E\|_{2,D}^* \leq C\mathcal{M}h^2 \left(\|F\|_{0,D} + |\alpha| + |\beta|\right), \tag{39}$$

holds with a constant C independent of h, F, α and β.

Proof. From Lemma 3.1, Lemma 2.1, (33) and (34), we can get (39) immediately. $\qquad\square$

Remark 3. From Theorem 3.2, we know that, $E(y) \equiv 0$ if $c(y)$ is a piecewise linear function, which implies that our method can get the exact solution in this case.

3.3. **Uniform convergence analysis for singular perturbation problem.** In this subsection, we will apply our TFPM to singular perturbation interface problem:

$$-\varepsilon U''(y) + c(y)U(y) = F(y), \quad \text{for } y \in D \setminus y_0, \tag{40}$$

$$U|_{\partial D} = 0, \tag{41}$$

$$[U]|_{y_0} = \alpha, \quad \left[\sqrt{\varepsilon}U'\right]\big|_{y_0} = \beta, \tag{42}$$

with $D = (0, d_0)$, $0 < \varepsilon \ll 1$ and

$$F \in L^2(D), \quad 0 < c_0 \leq c(x) \leq C_0 < +\infty, \quad \forall x \in D. \tag{43}$$

Let

$$\|v\|_{\varepsilon,D} = \sqrt{\varepsilon(|v|_{1,D}^*)^2 + |v|_{0,D}^2}. \tag{44}$$

Suppose that U is the solution of problem (40)–(42), and U_h is the solution of our TFPM. Let us define $E(y)$ and $R_h(y)$ as in (34), we then obtain

$$-\varepsilon E''(y) + c_h E(y) = R_h(y), \quad y \in D, \tag{45}$$

$$E(0) = 0, \qquad E(1) = 0, \tag{46}$$

$$E \quad \text{and} \quad E' \quad \text{are continuous on } D. \tag{47}$$

Then we have the *uniform convergence* of our TFPM for the singular perturbation problem.

Theorem 3.3. *The following error estimate*

$$\|E\|_{\varepsilon,D} \leq Ch^2 \left(\|F\|_{0,D} + |\alpha| + |\beta|\right), \tag{48}$$

holds with a constant C independent of ε, h, F, α and β.

Proof. Multiplying (40) by U and integrating over $D_1 \bigcup D_2$ yields

$$\varepsilon\alpha U'(y_0^-) + \sqrt{\varepsilon}\beta U(y_0^+) + \int_{D_1 \cup D_2} \left(\varepsilon|U'|^2 + c|U|^2\right) dy = \int_D FU \, dy.$$

By Young's inequality, we have

$$C\left(\|U\|_{\varepsilon,D}\right)^2 \leq \int_{D_1 \cup D_2} \left(\varepsilon|U'|^2 + c|U|^2\right) dy$$

$$= \int_D FU \, dy - \varepsilon\alpha U'(y_0^-) - \sqrt{\varepsilon}\beta U(y_0^+)$$

$$\leq \frac{1}{2\varepsilon_1}\|F\|_{0,D}^2 + \frac{\varepsilon_1}{2}\|U\|_{0,D}^2 + |\alpha| \cdot |\varepsilon U'(y_0^-)| + |\beta| \cdot |\sqrt{\varepsilon}U(y_0^+)|, \ \forall \varepsilon_1 > 0. \tag{49}$$

Furthermore, from the equation (40) and the conditions (43) and using Cauchy-Schwartz inequality and Young's inequality, we obtain

$$|\beta| \left| \sqrt{\varepsilon} U(y_0^+) \right| = |\beta| \left| \int_{d_0}^{y_0} \sqrt{\varepsilon} U'(y) \, dy \right| \leq |\beta| \int_{y_0}^{d_0} \left| \sqrt{\varepsilon} U'(y) \right| \, dy$$

$$\leq \sqrt{d_0 - y_0} |\beta| \cdot \sqrt{\varepsilon} |U|_{1,D_2} \leq \frac{1}{2\varepsilon_2} (d_0 - y_0)|\beta|^2 + \frac{\varepsilon_2}{2} \varepsilon |U|_{1,D_2}^2, \quad \forall \varepsilon_2 > 0,$$

$$|\alpha| \left| \varepsilon U'(y_0^-) \right| = \frac{|\alpha|}{y_0} \left| \int_0^{y_0} \varepsilon U'(y_0^-) dy \right|$$

$$= \frac{|\alpha|}{y_0} \left| \int_{D_1} \left(\varepsilon U'(y) + \int_y^{y_0} (cU - F)(z) \, dz \right) dy \right|$$

$$\leq \frac{|\alpha|}{y_0} \int_{D_1} \left| \varepsilon U'(y) + \int_y^{y_0} (cU - F)(z) \, dz \right| dy$$

$$\leq \frac{|\alpha|}{\sqrt{y_0}} \varepsilon |U|_{1,D_1} + |\alpha| \sqrt{y_0} \left(A_0 B_0 \|U\|_{0,D_1} + \|F\|_{0,D_1} \right)$$

$$\leq \frac{|\alpha|^2}{2y_0 \varepsilon_3} + \frac{\varepsilon_3 \varepsilon^2}{2} |U|_{1,D_1}^2 + \frac{|\alpha|^2 A_0^2 B_0^2 y_0}{2\varepsilon_4} + \frac{\varepsilon_4}{2} \|U\|_{0,D_1}^2 + \frac{|\alpha|^2 y_0 + \|F\|_{0,D_1}^2}{2},$$
$$\forall \, \varepsilon_3, \varepsilon_4 > 0.$$

Substituting the above inequalities into (49), choose $\varepsilon_1, \varepsilon_2, \varepsilon_3, \varepsilon_4$ small enough, we obtain

$$(\|U\|_{\varepsilon,D})^2 \leq C \left(\|F\|_{0,D}^2 + |\alpha|^2 + |\beta|^2 \right). \tag{50}$$

Similarly, by (45)–(47), we have

$$(\|E\|_{\varepsilon,D})^2 \leq C \left(\|R_h\|_{0,D} \right)^2 \leq Ch^2 \left(\|U\|_{0,D} \right)^2. \tag{51}$$

Then we get (48) from (50)–(51) immediately. $\qquad\square$
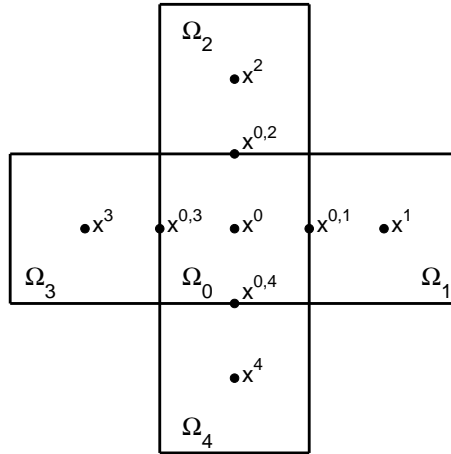

FIGURE 2. The location of points x^k and $x^{0,j}$, $k = 0, 1, \cdots, 4$, $j = 1, \cdots, 4$.

3.4. **Extension to two dimensional problems.** In this section, we shall construct some tailored finite point schemes for the interface problem in 2D:

$$-\Delta u(x) + c(x)u(x) = F(x), \quad \text{for } x = (x_1, x_2) \in \Omega \setminus \Gamma, \tag{52}$$

$$u\big|_{\partial\Omega} = 0, \quad [u]\big|_\Gamma = \alpha, \quad \left[\frac{\partial u}{\partial n}\right]\bigg|_\Gamma = \beta, \tag{53}$$

where $[v]|_\Gamma$ is the jump of a quantity v at the curve Γ,

$$F \in L^2(\Omega), \quad 0 < c_0 \le c(x) \le C < +\infty, \quad \forall x \in \Omega,$$

$$\Omega_0 \subset \Omega, \quad \Gamma = \partial\Omega_0, \quad \alpha \in H^{\frac{3}{2}}(\Gamma), \quad \beta \in H^{\frac{1}{2}}(\Gamma).$$

Taking a point $x^0 = (x_1^0, x_2^0)$ and four points around it

$$x^1 = (x_1^0 + 2h_1, x_2^0), \ x^2 = (x_1^0, x_2^0 + 2h_2), \ x^3 = (x_1^0 - 2h_3, x_2^0), \ x^4 = (x_1^0, x_2^0 - 2h_4),$$

where $h_i > 0, (i = 1, 2, 3, 4)$ are given (*cf.* Fig. 2). Then we approximate the coefficients $c(x)$ and the source term $F(x)$ by piecewise constants, *i.e.*

$$\left.\begin{array}{rcl} c(x) & \approx & \mu_j^2, \\ F(x) & \approx & F_j, \end{array}\right\} \quad x \in \Omega_j, \quad j = 0, 1, \cdots, 4.$$

We obtain the approximate problems in Ω_j,

$$-\Delta u + \mu_j^2 u = F_j, \quad x \in \Omega_j, \ j = 0, 1, \cdots, 4. \tag{54}$$

The solution of (54), $u(x)$, can be expanded at $x = x^j$ as:

$$u(x) = u_j(r) + a_0^j I_0(\mu r) + \sum_{n=1}^{\infty} \left(a_n^j I_n(\mu r) \cos n\theta + b_n^j I_n(\mu r) \sin n\theta\right), \tag{55}$$

where (r, θ) is the polar coordinates based on x^j, I_n is the n-th order modified Bessel function of first kind, and

$$u_j(r) = F_j \sum_{n=1}^{+\infty} \frac{(\mu_j)^{2n-2}}{4(n!)^2} r^{2n}. \tag{56}$$

We take the first few terms of the expansion of u at Ω_j $(j = 0, 1, 2, 3, 4)$,

$$u|_{\Omega_j} \approx u_j(r) + a_0^j I_0(\mu_j r) + I_1(\mu_j r)\left(a_1^j \cos\theta + b_1^j \sin\theta\right) + I_2(\mu_j r)a_2^j \cos 2\theta. \tag{57}$$

If the boundary of Ω_0 is not at the interface, we have the connected conditions

$$u \text{ and } \frac{\partial u}{\partial n} \text{ are continuous on the boundary of the cell } \Omega_0, \tag{58}$$

we then have

$$\begin{aligned} & u_0(h) + I_0(\mu_0 h)a_0^0 + I_1(\mu_0 h)a_1^0 + I_2(\mu_0 h)a_2^0 \\ = \ & u_1(h) + I_0(\mu_1 h)a_0^1 - I_1(\mu_1 h)a_1^1 + I_2(\mu_1 h)a_2^1, \\ & u_0'(h) + I_0'(\mu_0 h)a_0^0 + I_1'(\mu_0 h)a_1^0 + I_2'(\mu_0 h)a_2^0 \\ = \ & u_1'(h) + I_0'(\mu_1 h)a_0^1 - I_1'(\mu_1 h)a_1^1 + I_2'(\mu_1 h)a_2^1, \\[2mm] & u_0(h) + I_0(\mu_0 h)a_0^0 + I_1(\mu_0 h)b_1^0 - I_2(\mu_0 h)a_2^0 \\ = \ & u_2(h) + I_0(\mu_2 h)a_0^2 - I_1(\mu_2 h)b_1^2 - I_2(\mu_2 h)a_2^2, \\ & u_0'(h) + I_0'(\mu_0 h)a_0^0 + I_1'(\mu_0 h)b_1^0 - I_2'(\mu_0 h)a_2^0 \\ = \ & u_2'(h) + I_0'(\mu_2 h)a_0^2 - I_1'(\mu_2 h)b_1^2 - I_2'(\mu_2 h)a_2^2, \end{aligned}$$

$$u_0(h) + I_0(\mu_0 h)a_0^0 - I_1(\mu_0 h)a_1^0 + I_2(\mu_0 h)a_2^0$$
$$= u_3(h) + I_0(\mu_3 h)a_0^3 + I_1(\mu_3 h)a_1^3 + I_2(\mu_3 h)a_2^3,$$
$$u_0'(h) + I_0'(\mu_0 h)a_0^0 - I_1'(\mu_0 h)a_1^0 + I_2'(\mu_0 h)a_2^0$$
$$= u_3'(h) + I_0'(\mu_3 h)a_0^3 + I_1'(\mu_3 h)a_1^3 + I_2'(\mu_3 h)a_2^3,$$

$$u_0(h) + I_0(\mu_0 h)a_0^0 - I_1(\mu_0 h)b_1^0 - I_2(\mu_0 h)a_2^0$$
$$= u_4(h) + I_0(\mu_4 h)a_0^4 + I_1(\mu_4 h)b_1^4 - I_2(\mu_4 h)a_2^4,$$
$$u_0'(h) + I_0'(\mu_0 h)a_0^0 - I_1'(\mu_0 h)b_1^0 - I_2'(\mu_0 h)a_2^0$$
$$= u_4'(h) + I_0'(\mu_4 h)a_0^4 + I_1'(\mu_4 h)b_1^4 - I_2'(\mu_4 h)a_2^4.$$

The boundary conditions and the interface conditions (53) can be discretized directly too. Then we get a linear system of all the coefficients a_n^j and b_n^j. By solving this linear system, we can get the approximate solution immediately.

4. **Numerical studies.** In this section, we give some numerical examples to show the efficiency of our tailored finite point method.

Example 4.1. First, let us consider a simple problem

$$\begin{cases} -u''(x) + c(x)u(x) = 0, & x \in \Omega = (0,1), \\ u(0) = 0, \quad u(1) = 0, \\ [u]|_{\frac{1}{2}} = 1, \quad [u']|_{\frac{1}{2}} = 1; \end{cases} \tag{59}$$

with piecewise constant coefficient:

$$c(x) = \begin{cases} 1, & x \in \Omega_1 = (0, \frac{1}{2}), \\ 0, & x \in \Omega_2 = (\frac{1}{2}, 1). \end{cases}$$

The exact solution of problem (59) is

$$u(x) = \begin{cases} \frac{3\sqrt{e}}{3e-1}(e^{-x} - e^x), & x \in \Omega_1, \\ \frac{4}{3e-1}(1-x), & x \in \Omega_2. \end{cases}$$

In this case, we can use only three points, *i.e.* $h = \frac{1}{2}$, to get the exact solution by our tailored finite point method (*cf.* Table 1). We achieve the floating point relative accuracy. Here

$$E_{0,\infty}^{FP,h} = \max_{1 \le j \le 2} \|u - u_h^{FP}\|_{L^\infty(\Omega_j)}, \quad E_{1,\infty}^{FP,h} = \max_{1 \le j \le 2} \|u' - (u_h^{FP})'\|_{L^\infty(\Omega_j)},$$

$$E_{0,\infty}^{FV,h} = \max_{1 \le j \le 2} \|u - u_h^{FV}\|_{L^\infty(\Omega_j)}, \quad E_{1,\infty}^{FV,h} = \max_{1 \le j \le 2} \|u' - (u_h^{FV})'\|_{L^\infty(\Omega_j)},$$

where u_h^{FP} denotes the solution of our tailored finite point method with mesh size h, u_h^{FV} denotes the solution of standard second order finite volume method with mesh size h.

Example 4.2. Then, let us consider a problem

$$\begin{cases} -\big(a(x)u'(x)\big)' + b(x)u(x) = 0, & x \in \Omega = (0,1), \\ u(0) = 0, \quad u(1) = 0, \\ [u]|_{\frac{1}{2}} = 1, \quad [u']|_{\frac{1}{2}} = 1; \end{cases} \tag{60}$$

with piecewise smooth coefficient:

$$a(x) = \begin{cases} \frac{1}{2+4\sin^2 x}, & 0 < x < 0.5, \\ 0.5, & 0.5 < x < 1; \end{cases} \quad b(x) = \begin{cases} 10^3(1 + 2\sin^2 x), & 0 < x < 0.5, \\ 10^2(6x - \sin 2x), & 0.5 < x < 1. \end{cases}$$

TABLE 1. Example 4.1: L^∞ errors of different methods for different meshes.

mesh size h	1/2	1/4	1/8
$E_{0,\infty}^{FP,h}$	1.55E-15	1.55E-15	1.44E-15
$E_{1,\infty}^{FP,h}$	4.89E-15	5.33E-15	4.89E-15
mesh size h	1/10	1/20	1/40
$E_{0,\infty}^{FV,h}$	1.23E-3	3.13E-4	7.88E-5
$E_{1,\infty}^{FV,h}$	3.19E-3	8.13E-4	2.05E-4

In this case, the exact solution $u(x)$ of problem (60) can be got by (14)–(17). As $c(y) \equiv a\big(x(y)\big)b\big(x(y)\big)$ is a piecewise linear function of y, we can also get the exact solution by our TFPM (*cf.* Table 2) even if we use one point per subdomain. But because this problem has two interior layers at $x = \frac{1}{2}$, the standard finite difference scheme can not have good resolution if the mesh size is not small enough.

TABLE 2. Example 4.2: L^∞ errors of different methods for different meshes.

mesh size h	1/2	1/4	1/8
$E_{0,\infty}^{FP,h}$	5.22E-15	5.22E-15	4.77E-15
$E_{1,\infty}^{FP,h}$	5.99E-15	5.77E-15	5.55E-15
mesh size h	1/200	1/400	1/800
$E_{0,\infty}^{FV,h}$	5.47E-3	1.56E-3	4.17E-4
$E_{1,\infty}^{FV,h}$	3.48E-1	1.05E-1	2.84E-2

Example 4.3. Now, we consider a singular perturbation problem

$$\begin{cases} -\varepsilon\big(a(x)u'(x)\big)' + b(x)u(x) = f(x), & x \in \Omega = (0,1), \\ u(0) = 0, \quad u(1) = 0, \\ [u]|_{\frac{1}{4}} = -1, \quad [u']|_{\frac{1}{4}} = 1, \qquad [u]|_{\frac{1}{2}} = 1, \quad [u']|_{\frac{1}{2}} = 0; \end{cases} \tag{61}$$

with $0 < \varepsilon \ll 1$, $f(x) = \sin x$, and

$$a(x) = \begin{cases} 1+x, & 0 < x < \frac{1}{4}, \\ x, & \frac{1}{4} < x < \frac{1}{2}, \\ 1, & \frac{1}{2} < x < 1; \end{cases} \quad b(x) = \begin{cases} (1+\mathrm{e}^x), & 0 < x < \frac{1}{4}, \\ (1 - \ln x), & \frac{1}{4} < x < \frac{1}{2}, \\ 4, & \frac{1}{2} < x < 1. \end{cases}$$

In this case, the 'exact' solution $u(x)$ of problem (61) is solved by very fine mesh. Here

$$E_{r,2}^{FP,h} = \frac{\|u_h^{FP} - u\|_{r,\Omega}^*}{\|u\|_{r,\Omega}^*}, \qquad E_{r,2}^{FV,h} = \frac{\|u_h^{FV} - u\|_{r,\Omega}^*}{\|u\|_{r,\Omega}^*}, \quad r = 0, 1, 2,$$

$$E_{\varepsilon,\Omega}^{FP,h} = \frac{\|u_h^{FP} - u\|_{\varepsilon,\Omega}}{\|u\|_{\varepsilon,\Omega}}, \qquad E_{\varepsilon,\Omega}^{FV,h} = \frac{\|u_h^{FV} - u\|_{\varepsilon,\Omega}}{\|u\|_{\varepsilon,\Omega}}.$$

From Table 3, we find that we achieve the right convergence rate as shown in Theorem 3.2 although it has four interior layers near $x = \frac{1}{4}$ and $x = \frac{1}{2}$. In the contrast to this, we must use more discrete points to achieve the same accuracy for standard finite volume method. From Table 4, we find that we have the uniform convergence rate as shown in Theorem 3.3 whenever how small the ε is. In the

contrast to this, the corresponding errors of the standard finite volume method increase vary fast as ε becomes smaller and smaller, even we use very fine mesh.

TABLE 3. Example 4.3: Relative errors in different norms, $\varepsilon = 10^{-3}$.

mesh size h	$\frac{1}{16}$	$\frac{1}{32}$	$\frac{1}{64}$
$E_{0,2}^{FP,h}$	1.72E-3	4.25E-4	1.06E-4
$E_{1,2}^{FP,h}$	2.43E-3	5.95E-4	1.48E-4
$E_{2,2}^{FP,h}$	3.59E-3	9.03E-4	2.28E-4
mesh size h	$\frac{1}{160}$	$\frac{1}{320}$	$\frac{1}{640}$
$E_{0,2}^{FV,h}$	3.08E-3	8.36E-4	2.19E-4
$E_{1,2}^{FV,h}$	9.61E-3	2.66E-3	6.85E-4
$E_{2,2}^{FV,h}$	7.89E-2	3.37E-2	8.41E-3

TABLE 4. Example 4.3: Relative errors for different ε, here $h_1 = \frac{1}{16}$, $h_2 = \frac{1}{640}$.

ε	10^{-4}	10^{-5}	10^{-6}
$E_{\varepsilon,\Omega}^{FP,h_1}$	3.74E-3	7.92E-3	8.33E-3
$E_{\varepsilon,\Omega}^{FV,h_2}$	2.36E-3	1.41E-2	1.93E-1

Example 4.4. Now we consider a mixed elliptic-hyperbolic problem

$$\begin{cases} -u''(x) + c(x)u(x) = 0, & x \in \Omega = (0,1), \\ u(0) = 0, \quad u'(1) - i60\pi u(1) = 0, \\ [u]|_{\frac{1}{4}} = 0, \quad [u']|_{\frac{1}{4}} = -1, \quad [u]|_{\frac{1}{2}} = 0, \quad [u']|_{\frac{1}{2}} = 10; \end{cases} \quad (62)$$

with

$$c(x) = \begin{cases} 2x^2, & 0 < x < \frac{1}{4}, \\ 10000 - 40000x^2, & \frac{1}{4} < x < \frac{1}{2}, \\ -4800\pi^2(x^2 - \frac{1}{4}), & \frac{1}{2} < x < 1. \end{cases}$$

When $x < \frac{1}{2}$, the problem (62) is an elliptic problem. But it is a Helmholtz equation when $x > \frac{1}{2}$. In this case, the 'exact' solution $u(x)$ of problem (61) is solved by very fine mesh. From Table 5, we find that we achieve the right convergence rate as shown in Theorem 3.2. Actually, in Figure 3, we can not distinguish the exact solution and our approximate solution by TFPM even we only use eight points in the whole computational domain Ω. On the other hand, we must use much more discrete points to achieve the same accuracy for standard finite volume method.

Example 4.5. Finally, we consider a two-dimensional problem

$$\begin{cases} -\Delta u(x) + c(x)u(x) = 0, & x \in \Omega = (-1,1) \times (-1,1), \\ u|_{\Gamma_1} = 0, \quad u|_{\Gamma_2} = 1 - x_1, \\ [u]|_\Gamma = 1, \quad [u']|_\Gamma = 0; \end{cases} \quad (63)$$

TABLE 5. Example 4.4: Relative errors in different norms.

mesh size h	$\frac{1}{16}$	$\frac{1}{32}$	$\frac{1}{64}$
$E_{0,2}^{FP,h}$	4.26E-2	1.03E-2	2.60E-3
$E_{1,2}^{FP,h}$	7.31E-2	1.84E-2	4.63E-3
$E_{2,2}^{FP,h}$	8.02E-2	2.01E-2	5.08E-3
mesh size h	$\frac{1}{160}$	$\frac{1}{320}$	$\frac{1}{640}$
$E_{0,2}^{FV,h}$	6.23E-1	1.46E-1	4.04E-2
$E_{1,2}^{FV,h}$	9.34E-1	2.36E-2	6.51E-2
$E_{2,2}^{FV,h}$	1.211	2.99E-1	7.91E-2

Real part (left) and imaginary part (right) of solutions. $(h = \frac{1}{8})$

Real part (left) and imaginary part (right) of solutions. $(h = \frac{1}{16})$
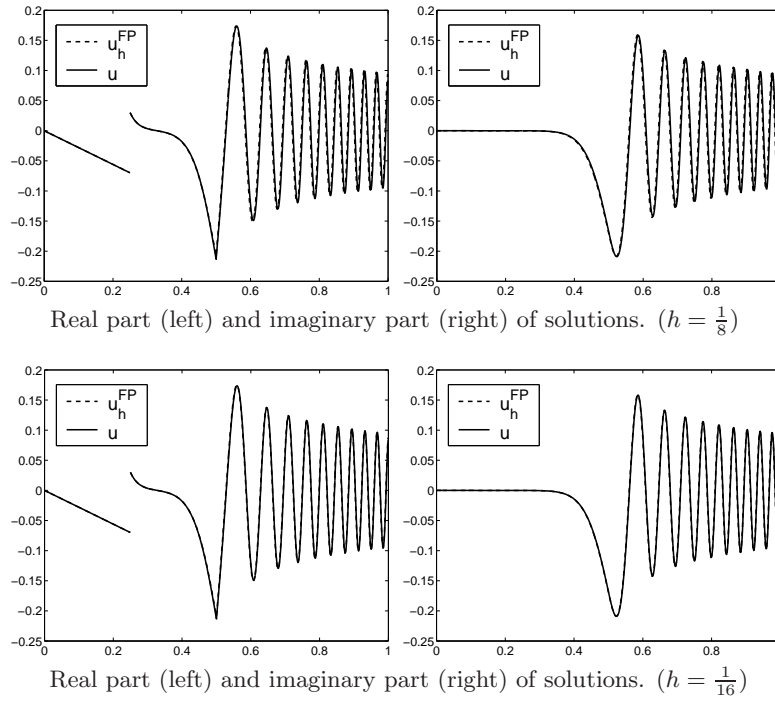
FIGURE 3. The numerical solutions for example 4.4.

with

$$\Gamma = \left\{ (x_1, x_2) \in \mathbb{R}^2 \mid -1 \leq x_2 \leq 1, x_1 = 0 \right\},$$
$$c(x) = \begin{cases} 4, & x_1 < 0, \\ 1, & x_1 > 0; \end{cases}$$

and

$$\begin{aligned}
\Gamma_1 \quad &= \quad \left\{ (x_1, x_2) \in \mathbb{R}^2 \,\middle|\, -1 \le x_2 \le 1, x_1 = \pm 1 \right\} \\
&\bigcup \quad \left\{ (x_1, x_2) \in \mathbb{R}^2 \,\middle|\, -1 \le x_1 < 0, x_2 = \pm 1 \right\}, \\
\Gamma_2 \quad &= \quad \left\{ (x_1, x_2) \in \mathbb{R}^2 \,\middle|\, 0 < x_1 \le 1, x_2 = \pm 1 \right\}.
\end{aligned}$$

The results for $h = 1/32$ and $h = 1/64$ are given in Figure 4. From this figure, we can see that our method are also very effective in two dimensional case.
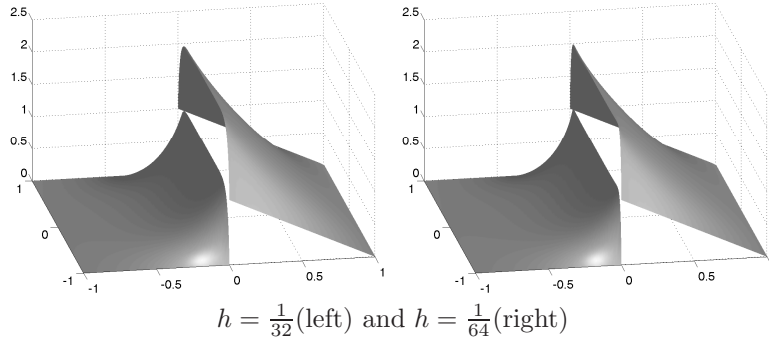

$$h = \tfrac{1}{32}(\text{left}) \text{ and } h = \tfrac{1}{64}(\text{right})$$

FIGURE 4. The numerical solutions for example 4.5.

5. **Conclusion.** In this paper, we present a *tailored finite point* method for the elliptic equation with discontinuous coefficients and jump conditions. First, we make a coordinates transform and approximate the coefficient $c\big(x(y)\big) = a\big(x(y)\big)b\big(x(y)\big)$ by piecewise linear polynomials. Then we solve the locally approximate problems to get a local basis. Finally, we get the approximate solution by the expansion of this basis. Our finite point method has been tailored to some particular properties of the problem. Therefore, our approximate solution has almost the same behaviors of the exact solution. In particular, when the coefficient $c(y)$ is a piecewise linear function, we can get the *exact solution* with only one point in each subdomain. Our method has a fast solver where the computational complexity is only $O(N)$ with N discrete points. Our convergence analysis also proves that our method has the *second order convergent rate* in the second order energy norm $\|\cdot\|_{2,\Omega}^*$. The numerical results show that we can get very good approximations even though we only use a few points, whenever the interface problems have what kinds of singularities and what kind of interior layers (*cf.* examples 4.1–4.3). Even for a mixed elliptic-hyperbolic problem (*cf.* example 4.4), our TFPM still has high accuracy although the interface problem has two elliptic regions with interior layers and a hyperbolic region with high wave number. As our method works so efficiently in different kinds of interface problems in 1D and 2D, we can extend it to more complicated and high dimensional problems towardly.

<div align="center">REFERENCES</div>

[1] I. Babuška, *The finite element method for elliptic equations with discontinuous coefficients*, Computing, **5** (1970), 207–213.

[2] I. Babuška, *Solution of problems with interface and singularities*, Tech. Note BN-789, Institute for Fluid Dynamics and Applied Mathematics, University of Maryland, 1974.

[3] I. Babuška, G. Caloz and J. E. Osborn, *Special finite element methods for a class of second order elliptic problems with rough coefficients*, SIAM J. Numer. Anal., **31** (1994), 945–981.

[4] J. W. Barrett and C. M. Elliott, *Fitted and unfitted finite-element methods for elliptic equations with smooth interfaces*, IMA J. Numer. Anal., **7** (1987), 283–300.

[5] A. E. Berger, H. D. Han and R. B. Kellogg, *A priori estimates and analysis of a numerical method for a turning point problem*, Math. Comp., **42** (1984), 465–492.

[6] Z. Chen and J. Zou, *Finite element methods and their convergence for elliptic and parabolic interface problems*, Numer. Math., **79** (1998), 175–202.

[7] M. Cheng and G. R. Liu, *A novel finite point method for flow simulation*, Int. J. Numer. Meth. Fluids, **39** (2002), 1161–1178.

[8] R. B. Kellogg, *Singularities in interface problems*, in "Numerical Solution of Partial Differential Equations II" (eds. B. Hubbard.), New York, Academic Press, 1971.

[9] B. Kellogg, *On the poisson equation with intersecting interfaces*, Applicable Anal., **4** (1974/75), 101–129.

[10] H. Han, *The numerical solutions of the interface problems by infinite element methods*, Numer. Math., **39** (1982), 39–50.

[11] H. Han and Z. Huang, *A tailored finite point method for the Helmholtz equation with high wave numbers in heterogeneous medium*, J. Comp. Math., **26** (2008), 728–739.

[12] H. Han, Z. Huang and R. B. Kellogg, *A tailored finite point method for a singular perturbation problem on an unbounded domain*, J. Sci. Comp, **36** (2008), 243–261.

[13] A. M. Il'in, *Differencing scheme for a differential equation with a small parameter affecting the highest derivative*, Math. Notes, **6** (1969), 596–602.

[14] R. J. LeVeque and Z. L. Li, *The immersed interface method for elliptic equations with discontinuous coefficients and singular sources*, SIAM J. Numer. Anal., **31** (1994), 1019–1044.

[15] Z. L. Li and K. Ito, *Maximum principle preserving schemes for interface problems with discontinuous coefficients*, SLAM J. Sci. Comput., **23** (2001), 339–361.

[16] Z. Li and K. Ito, "The Immersed Interface Method: Numerical Solutions of PDEs Involving Interfaces and Irregular Domains," SIAM Frontiers in Applied Mathematics, **33**, Philadelphia, 2006.

[17] H. Lin and S. N. Atluri, *The meshless local petrov-galerkin(mlpg) method for solving incompressible navier-stokes equations*, CMES, **2** (2001), 117–142.

[18] B. Mendez and A. Velazquez, *Finite point solver for the simulation of 2-D laminar incompressible unsteady flows*, Comput. Methods Appl. Mech. Engrg., **193** (2004), 825–848.

[19] J. J. H. Miller, *On the convergence, uniformly in ε, of difference schemes for a two-point boundary singular perturbation problem*, Numerical Analysis of Singular Perturbation Problems (eds. Hernker P. W. and Miller J. J, H.), Academi Press, 467–474, 1979.

[20] E. Oñate, S. Idelsohn, O. C. Zienkiewicz and R. L. Taylor, *A finite point method in computational mechanics, applications to convective transport and fluid flow*, Int. J. Numer. Methods Engrg., **39** (1996), 3839–3866.

[21] R. K. Sinha and B. Deka, *An unfitted finite-element method for elliptic and parabolic interface problems*, IMA J. Numer. Anal., **27** (2007), 529–549.

[22] S. Yu, Y. Zhou and G. W. Wei, *Matched interface and boundary (MIB) method for elliptic problems with sharp-edged interfaces*, J. Comput. Phys., **224** (2007), 729–756.

[23] Y. C. Zhou, S. Zhao, M. Feig and G. W. Wei, *High order matched interface and boundary method for elliptic equations with discontinuous coefficients and singular sources*, J. Comput. Phys., **213** (2006), 1–30.

E-mail address: `zhuang@math.tsinghua.edu.cn`